Discrete element method for generating random fibre distributions in micromechanical models of fibre reinforced composite laminates

Yaser Ismail[a], DongminYang[b,*], Jianqiao Ye[a,*]

[a] Department of Engineering, Lancaster University, Lancaster LA1 4YW, UK

[b] School of Civil Engineering, University of Leeds, Leeds LS2 9JT, UK

Abstract

A new approach is presented for generating random distribution of fibres in the representative volume element (RVE) of fibre reinforced composite laminates. The approach is based on discrete element method (DEM) and experimental data of fibre diameter distribution. It overcomes the jamming limit appeared in previous methods and is capable of generating high volume fractions of fibres with random distributions and any specified inter-fibre distances. Statistical analysis is then carried out on the fibre distributions generated within the RVEs, which show good agreement with experiments in all statistics analysed. The effective elastic properties of the generated RVEs are finally analysed by finite element method, which results show more reasonable agreement with the experimental results than previous methods.

Keywords: Fibre reinforced composites; Micromechanical modelling; Discrete element method; Representative volume element

1. Introduction

Fibre reinforced composite laminates have been widely used in the aerospace industry due to their excellent material properties such as high stiffness, high strength and light weight. These applications require extremely high confidence in the structural integrity of composite laminates which in turn has urged the demand of more accurate computational tools to predict their mechanical behaviour including failure strength. Composite laminates can fail as a result of several damage modes taking place at different scales, namely fibre breakage, fibre/matrix debonding and matrix cracking at microscale and delamination at macroscale. To capture all those damage events across different scales, multi-scale modelling approach has been attempted, in which the information of deformation and failure of a micromechanical model is fed into a macro-mechanical model for predicting the structural behaviour of the entire composite [1, 2].

In the conventional micromechanical analysis of composites with detailed microstructures, fibres are usually arranged in a periodic pattern within a composite. A single unit cell model, *i.e.*, a simpler Representative Volume Element (RVE), can then be produced with one or a few fibres regularly distributed within a ply. For example, Parıs *et al.*,[3] used a single fibre unit cell model to study interface debonding. Using a

*Corresponding authors. Emails: d.yang@leeds.ac.uk (D Yang); j.ye2 @lancaster.ac.uk(J Ye).

similar technique Correa *et al*., [4] investigated the initiation and propagation of interface cracks. This assumption reduces the computational cost whilst still can precisely predict the effective elasticity of a single layer composite material. However, the single unit cell model does not reflect the reality that composite materials in fact have irregular distribution of fibres, thus cannot perform well when it is applied to predict the failure behaviour [5, 6]. Gusev *et al*.,[7] found that random distribution of fibres had a considerable effect on the transverse elasticity. Trias *et al*., [8] carried out the stress and strain analysis in both periodic and random models for carbon fibre reinforced composites, and concluded that periodic models might underestimate matrix cracking and damage initiation. This was also evidenced from the stress analysis by Hojo*et al*.,[9] who found that the normal interfacial stresses were affected by the inter-fibre distance and the stresses increased rapidly when the distance was less than 0.5 μm.

Several approaches have been reported in the literature for generating statistically equivalent RVEs (SERVEs) of composite materials with non-uniform distributions of fibres. A SERVE has the smallest volume size but can still maintain the same stress-strain relationship as that of the entire composite [5]. Usually the hard-core model (also called random sequential absorption model) was used to generate a SERVE. In a 2D hardcore model the fibres are represented by discs randomly distributed in a square domain without any overlap. The hard-core model is natural and simple, and its only disadvantage is that it has difficulties in generating a random distribution of fibres with a volume fraction higher than 50% due to a jamming limit [10]. This limitation was later eliminated by Wongsto and Li [11] who proposed a method that generated random distribution by shaking an initial hexagonal packing of the fibres. Therefore this approach was also called initially periodic shaking model (IPSM) [12]. However, no statistics analysis was performed on this algorithm and the initial periodic arrangement might not be fully changed by the shaking procedure. Melro *et al*.,[13] developed a hard-core shaking model (HCSM) in which the classical hard-core model was used to generate an initial fibre distribution and then small arbitrary displacements were assigned to the fibres to enable random motions. During the process matrix rich regions were created in certain areas where more fibres could be placed in order to achieve higher volume fractions. Because the hard-core model involves uncertainties in generating the initial configuration, it requires a relatively complex algorithm for the fibres to move. A simpler algorithm, random sequential expansion (RSE), was recently developed by Yang *et al*., [12]. The algorithm was still based on hard-core model and the inter-fibre distances were controllable. However, the fibre diameters in this algorithm were assumed to be uniform, and the inter-fibre distance had to be zero in order to achieve a volume fraction of 68%. This zero inter-fibre distance could cause numerical difficulties when analysing RVE using FEM because there has to be a sufficient distance between two neighbouring fibre surfaces to ensure adequate elements to cover those areas as matrix [14].

Besides the above mentioned numerical approaches, there are also some experimental image based models. The idea of those models is to obtain digital images of transverse

sections using scanning electronic microscopic (SEM) or high-resolution optical microscopic and then use a computer software to locate the fibre centroids by detecting a colour 'threshold' of the fibres. For instance, Vaughan and McCarthy [15] measured the diameter distribution and used a nearest neighbour algorithm (NNA) to define the inter-fibre distances for generating a SERVE of high strength composite laminates. The obvious benefit of image-based method is that it can be used to generate a microstructure exactly the same as the original cross section area of the composite material. However, this is time-consuming and requires specific computer software to process the images in order to identify the locations of the fibres.

This paper presents a new algorithm which combines experimental and IPSM models and uses the discrete element method (DEM) to generate random distributions of fibres. Experimentally measured fibre diameter distribution is adopted in DEM for generating fibres of different size that are, initially, in a regular arrangement. IPSM approach is then used in DEM to create randomness of fibre location. High fibre volume fraction is achieved by easily adding additional particles in DEM. Statistical functions are used to analyse the generated fibre distributions with comparisons to the previous approaches in [12, 15]. The configuration of fibres is then transferred to FEM models to investigate the effective elasticity of the microstructures generated using the DEM approach, which shows a good prediction of the material's transversal isotropy. The developed algorithm is based on DEM thus it provides a natural advantage for future DEM micromechanical modelling. Also, the algorithm can be easily combined with conventional FEM micromechanical modelling.

2. Algorithm development using DEM

In this section an algorithm is developed in DEM to generate random distributions of fibres with high volume fractions, which improves the previous one proposed by the authors in [16] by combining experimental and shaking approaches.

In our previous work [16] fibres diameters were assumed to be identical which resulted in almost constant inter-fibre distances. To overcome this issue, variable fibre diameters were drawn from the experimentally measured data and used for fibre generation in DEM software package PFC2D [17]. The diameters of the fibre in this study conform to normal distribution with mean fibre diameter of 6.6 μm and standard deviation of 0.3106 [15], as shown by the solid curve in Fig.1. The fibre volume fraction used in this case is 60%, the same as used in [15]. The new method is explained bellow and illustrated in Fig.2.

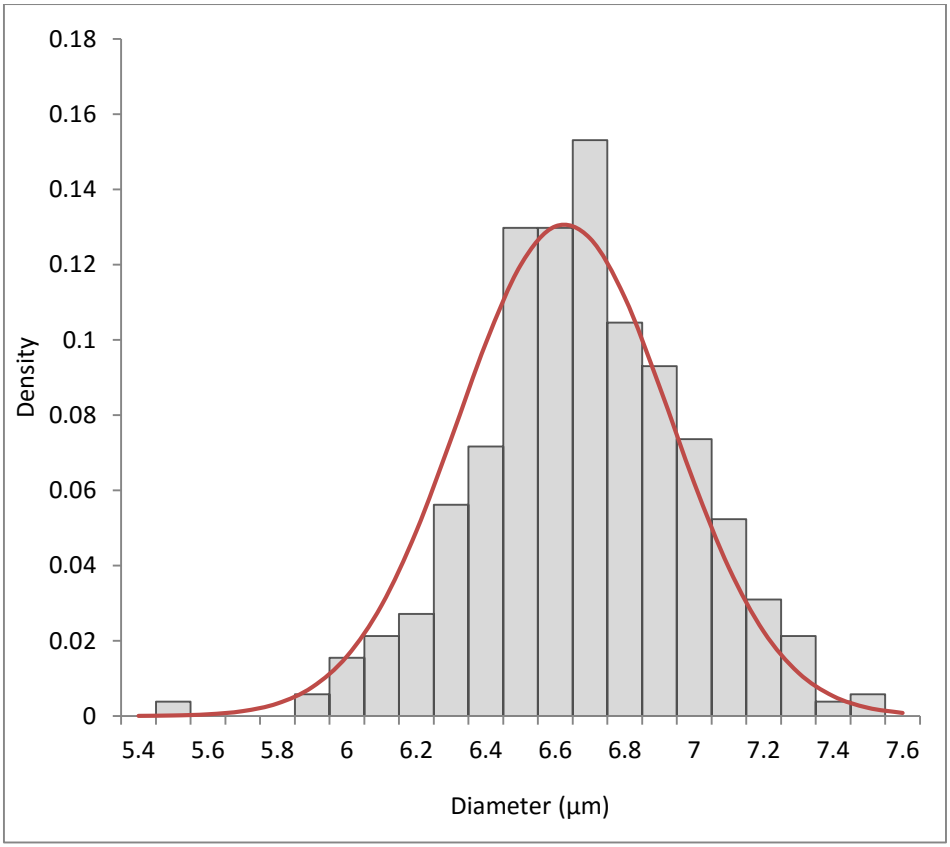

Fig.1. Size distribution of fibres.

(i) Using the mean fibre diameter $\overline{D}_f$, the required number of fibres, N_f, is approximately determined by the following simple calculation:

$$N_f = \frac{4V_f L^2}{\pi \overline{D}_f^2} \tag{1}$$

Once the number of fibres is known, a random number, α, between -1 and 1 is created in DEM software PFC2D and used to calculate the diameter of each fibre to be generated, D_f, following the Gaussian normal distribution function:

$$D_f = \overline{D}_f + \alpha\delta_f \tag{2}$$

In the 2D DEM modelling, each fibre is represented by a disc in PFC2D. The diameter distribution of discs/fibres in the DEM model is also plotted in Fig .1, which matches the distribution function extracted from experimental data. The discs/fibres are initially placed in a regular cubic arrangement, as shown in Fig.2a.

(ii) Since the fibre diameters are not identical, in some cases the resultant fibre volume fraction could be smaller than the target fibre volume fraction. Therefore, more discs/fibres are added one by one in random places and overlap with those generated earlier in order to achieve the target volume fraction, as shown in Fig.2b. The instant

volume fraction is re-calculated after every single disc is added, and the process terminates when the target fibre volume fraction is reached.

(iii) Random velocity is applied simultaneously to each of the discs that moves in a way similar to the Brownian motion. The motion of the discs is governed by the Newton's Second Law and the collisions between any two discs are according to a Hertz contact law [16, 17]. In this step there are two major groups of discs, as shown in Fig. 3b. The grey ones are the internal discs staying within the RVE, and the red ones are those moving across the RVE boundary from the inside. As a consequence of the motion of the red discs, the fibre volume fraction of the RVE is reduced. To compensate this loss and maintain the initial fibre volume fraction, paired discs, denoted by the blue ones, are added along the opposite boundary mapping the respective positions of the red outgoing red discs. This is achieved using periodic boundary condition available in PFC2D [17]. The velocity of each disc is then set to zero after a sufficient period of time of free motion, and the whole model gradually reaches a static equilibrium state.

(iv) At this stage, there might exist overlaps between some discs, while in reality there are normally small distances between fibre surfaces. To resolve this issue, the radii of all the discs are increased by half of the minimum required distance between two neighbouring fibre surfaces [16]. By Hertz contact law, there will be repulsive forces at the contact between any two particles with an overlap to produce relative displacement and consequently increase the distance between them. After this additional redistribution, the whole model reaches an equilibrium state again and the radii of all the discs are reduced back to their initial values.

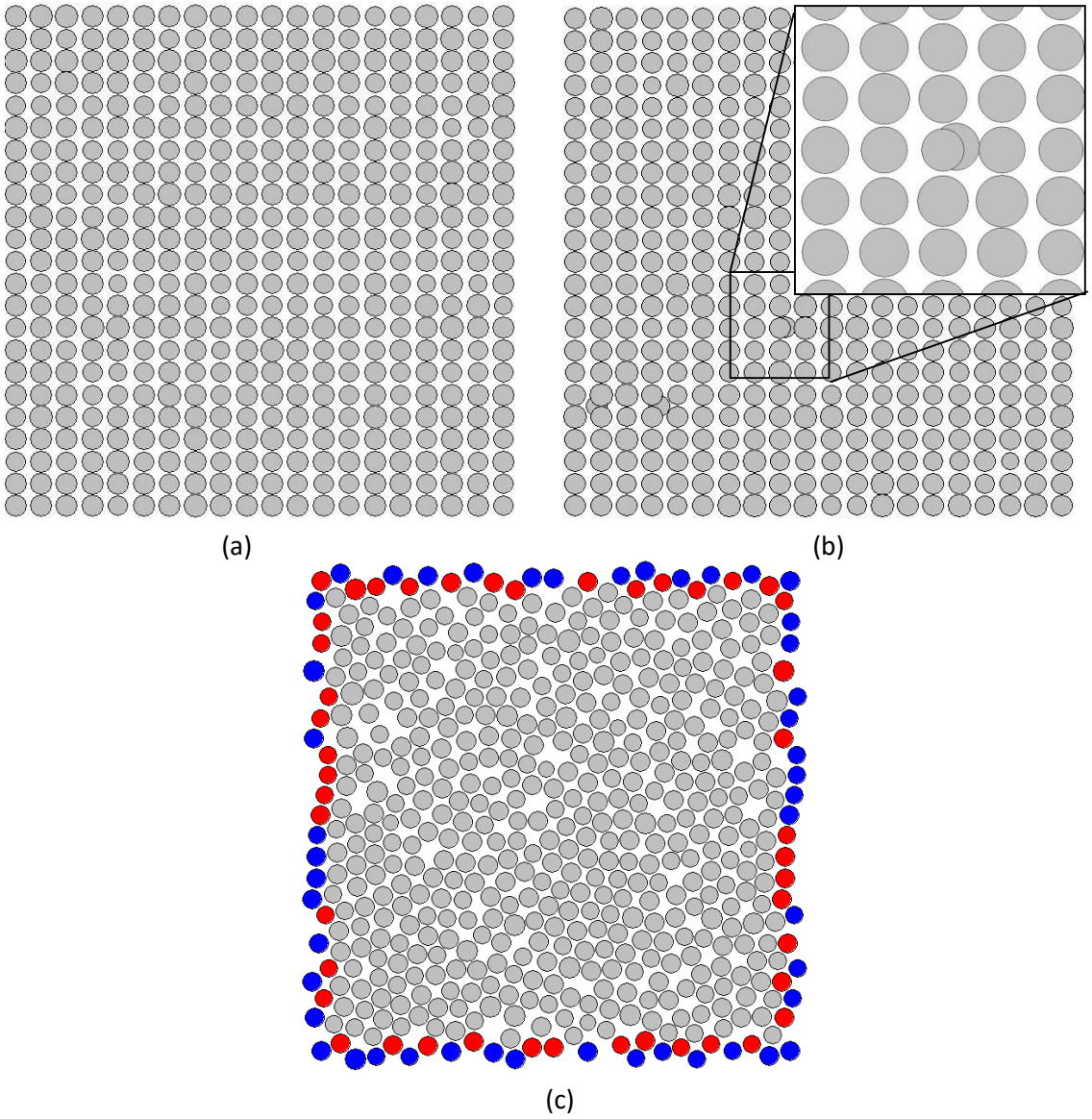

Fig.2. Procedure for generating random fibre distributions using DEM. (a) Initial fibre distribution in regular cubic arrangement. (b) More discs are added in. (c) Periodic boundary condition is applied to maintain the constant fibre volume fraction.

This algorithm can be used to generate high fibre volume fractions with any specified inter-fibre distances. Examples of fibre distributions with fibre volume fractions of 60%, 65% and 68%, and a minimum inter-fibre distance of 0.8μm are shown in Fig.3. The results have demonstrated that the presented algorithm is capable of generating microstructures of composites with required high fibre volume fractions.

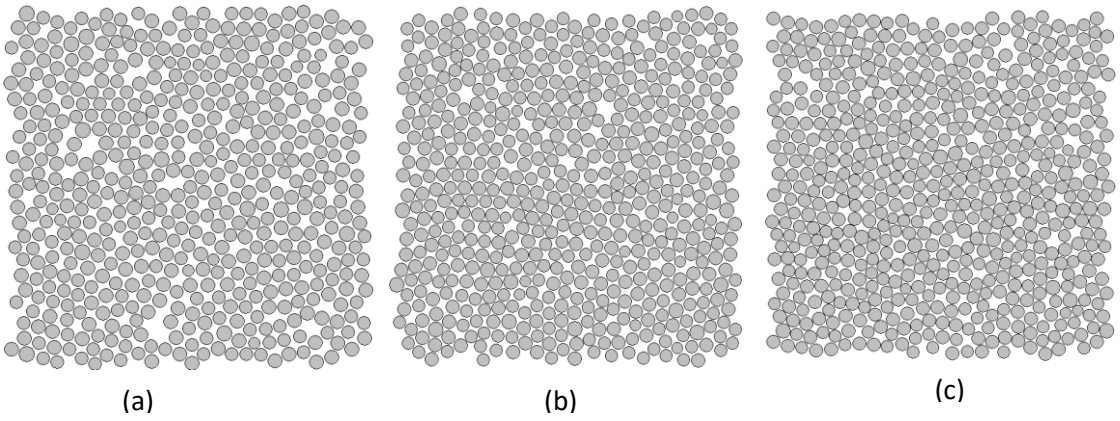

Fig.3. Three fibre distributions with high volume fractions: (a) 60%, (b) 65%, and (c) 68%.

3. Statistical characterisation

This section is dedicated to the statistical analysis of the fibre distributions generated by the present algorithm. The statistical methods employed here are normally used to quantitatively describe the random point distributions in the space. For the purpose of comparison, exactly the same statistical descriptors used in [12, 15] are adopted in this study and the positions of all fibres are considered as a spatial point pattern [18].

Four statistical descriptors are adopted, *i.e.*, nearest neighbour distribution function, cumulative distribution function, second-order intensity function and pair distribution function. Several parameters are considered such as the side length of RVE, L, volume fraction, V_f and fibre radius, r_f. The RVE size can be described by the variable δ, which defines the relationship between the side length of RVE and the fibre radius as:

$$\delta = \frac{L}{r_f} \tag{3}$$

The size of RVE needs to be sufficiently large to characterise the behaviour of a bulk material. For a typical composite material such as carbon fibre reinforced polymer (CFRP) with a fibre volume fraction of 50%, Trias *et al.*, [19] found that the minimum size of RVE was δ=50. The values used for the input variables in this study were same as those used in [12, 13, 15], *i.e.*, δ=50, V_f=60% and the fibre diameters were obtained from a normal distribution. A total of twenty-five RVEs were generated and each of them had the same size of 165 μm × 165 μm. Results of the four statistical functions were compared with the experimental data reported by Vaughan and McCarthy [15] and the recent RSE algorithm proposed by Yang *et al.*,[12]. MATLAB [20] was used to calculate all statistical descriptors explained later in this section.

3.1 Nearest neighbour distribution

As one of the basic functions to characterise a system of interacting points in the space, nearest neighbour distribution is defined as the probability density of finding a nearest

neighbour of a reference point. Therefore it can be used as an indicator to assess whether the fibres in a RVE are random, regular or clustered. Fig.4a and 4b show the results of the 1st and 2nd nearest neighbour distributions of twenty-five RVEs, respectively. Error bars are included in the figures to indicate the variation of data at each point. For comparisons the experimental and RSE results are also plotted in the figures. It is evident that the results from the present method show better comparison with the experimental distribution than the ones of RSE [12]. Furthermore, the short range interaction of fibres is very close to the experimental data. This minimal spacing between fibres is particularly important and has been found to have a significant influence on the failure mechanism of composite materials as the peak stresses normally appear in the area where fibres are close to each other [9].

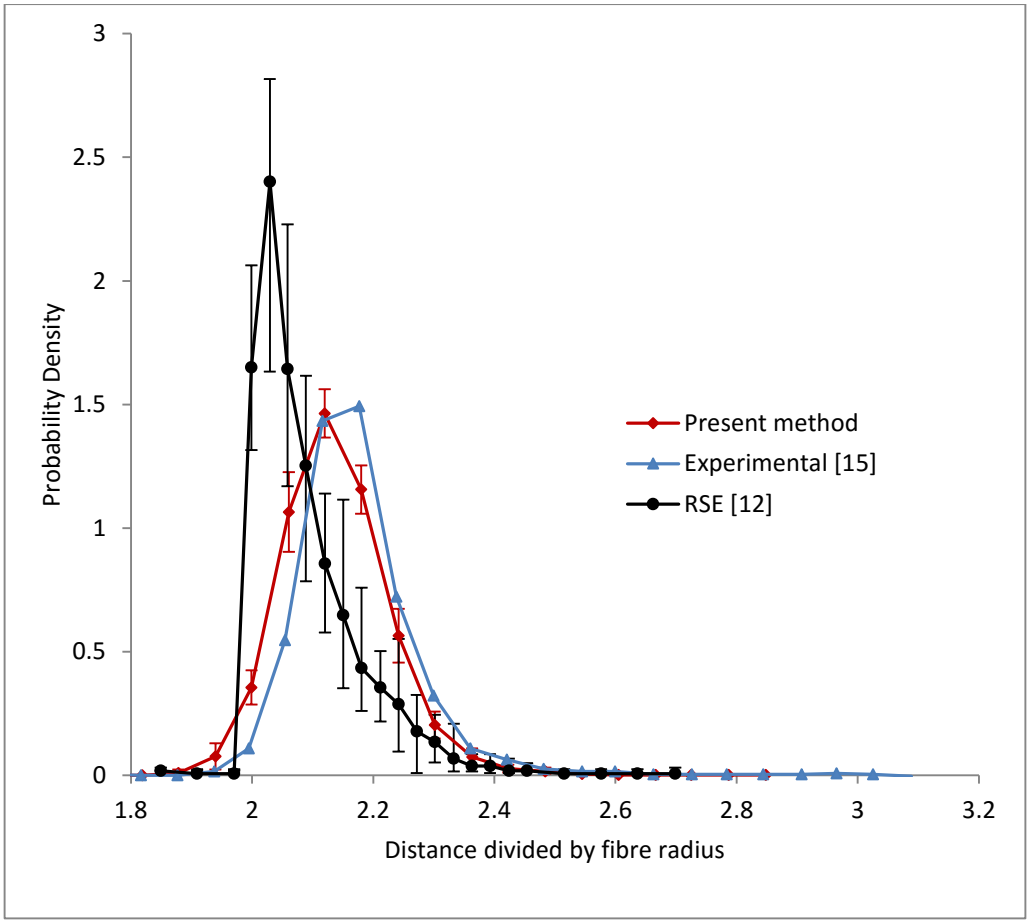

(a)

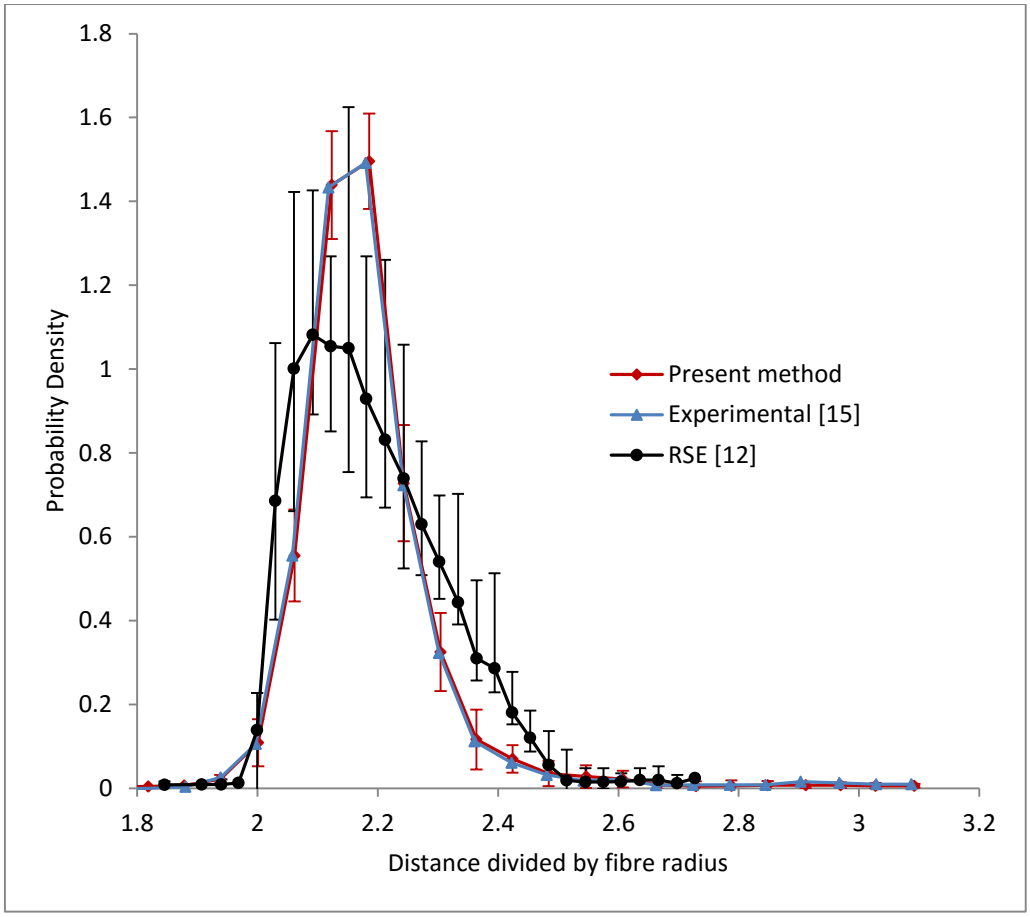

(b)

Fig.4. Results of near neighbour distributions compared with experimental data and RSE results. (a) 1st Nearest neighbour distribution. (b) 2nd Nearest neighbour distribution function.

3.2 Second-order intensity function

The second-order intensity function, also called Ripley's *K* function, is another statistical tool that has been extensively used to analyse a spatial pattern [21]. The function is defined as the number of more points to be added within a radial distance, *r*, of an arbitrary point divided by the number of points per unit area, *n*. Unlike the 1st and 2nd nearest neighbour distributions which depend on the local information of the points, the edge of the domain, *w*, and overlap effects are taken into account by the Ripley' *K* function because they have a significant effect when calculating this function. The Ripley's *K* function is estimated by:

$$K(r) = \frac{A}{N^2}\sum_{i}\sum_{i\neq j}\omega_{ij}^{-1} I(\mathrm{r_{ij}} \le \mathrm{r}), \tag{4}$$

where *A* is the area of the domain, *N* is the total number of points in the domain, *I*(.) is the indicator function, r_{ij} is the distance between points *i* and *j*, and ω_{ij} is the ratio of the circumference contained within the domain to the whole circumference of the circle r_{ij}. Point fields are usually compared with the complete spatial randomness (CSR) pattern, and the Ripley's *K* function computed by [18]:

$$K(r) = \pi r^2. \quad (5)$$

The comparison between the shape of *K(r)* and the shape of CSR patterns provides important information for assessing the fibre distribution. For instance, when the *K(r)* curve of is below the CSR curve , it gives an indication that the distribution is somehow regular, otherwise it means that some fibres are clustered in the area [13]. Shown in Fig.5 are the mean second-order intensity functions for twenty-five RVEs generated using the present method, experimental, RSE and CSR results. The results can be split into two areas. When distances are shorter (*i.e.*, $r \leq 15$), the curve obtained from the present work is close and above the experimental and both show stair-shape-likes, as shown in the zoom-in view of Fig.5. The curve is also above the CSR, which indicates the fibre distribution is regular at these distances as explained above, but it is gradually separating from the other two at larger distances (*i.e.*,$r > 15$), as a result of the long range clustering.

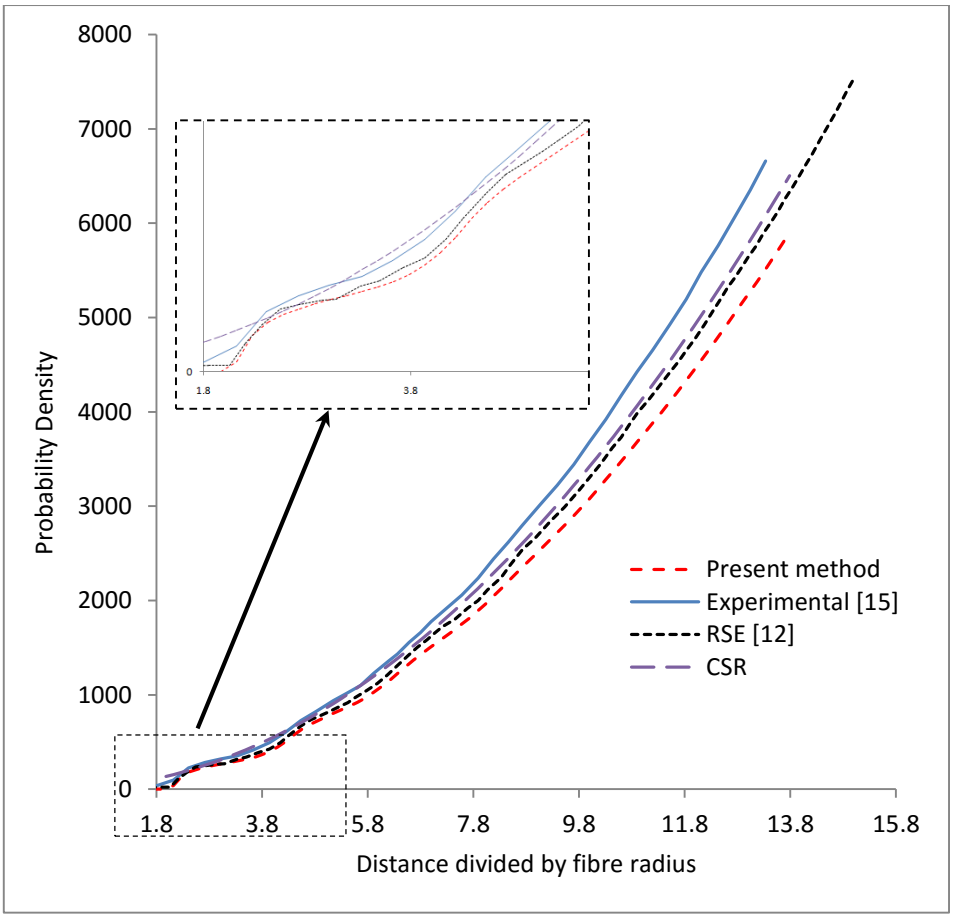

Fig.5. Second-order intensity function, compared with experimental, RSE method and CSR.

3.3 Radial distribution function

The radial distribution function is an important statistical tool that is mostly used to study a system of particles such as atoms or molecules. The function describes the

change of the average fibre density as a function of distance from a reference point which, in our case, is a given fibre centre. It is mathematically defined as [5]:

$$g(r) = \frac{1}{2\pi r}\frac{\mathrm{d}K(r)}{\mathrm{d}r}, \tag{6}$$

where *g(r)* is the intensity of the fibre distances and *K(r)* is the second-intensity function . Fig.6 shows the mean radial distribution functions for the microstructures generated by the present DEM method, together with the experimental and RSE microstructures. Again, excellent agreement is found between the present method and experimental data and this can be seen at larger distances when both tend to 1, which confirms the randomness distributions of fibres. Therefore, it is proved that the developed algorithm using DEM is a useful tool for generating random fibre distributions in RVEs of composite materials for micromechanical analysis.

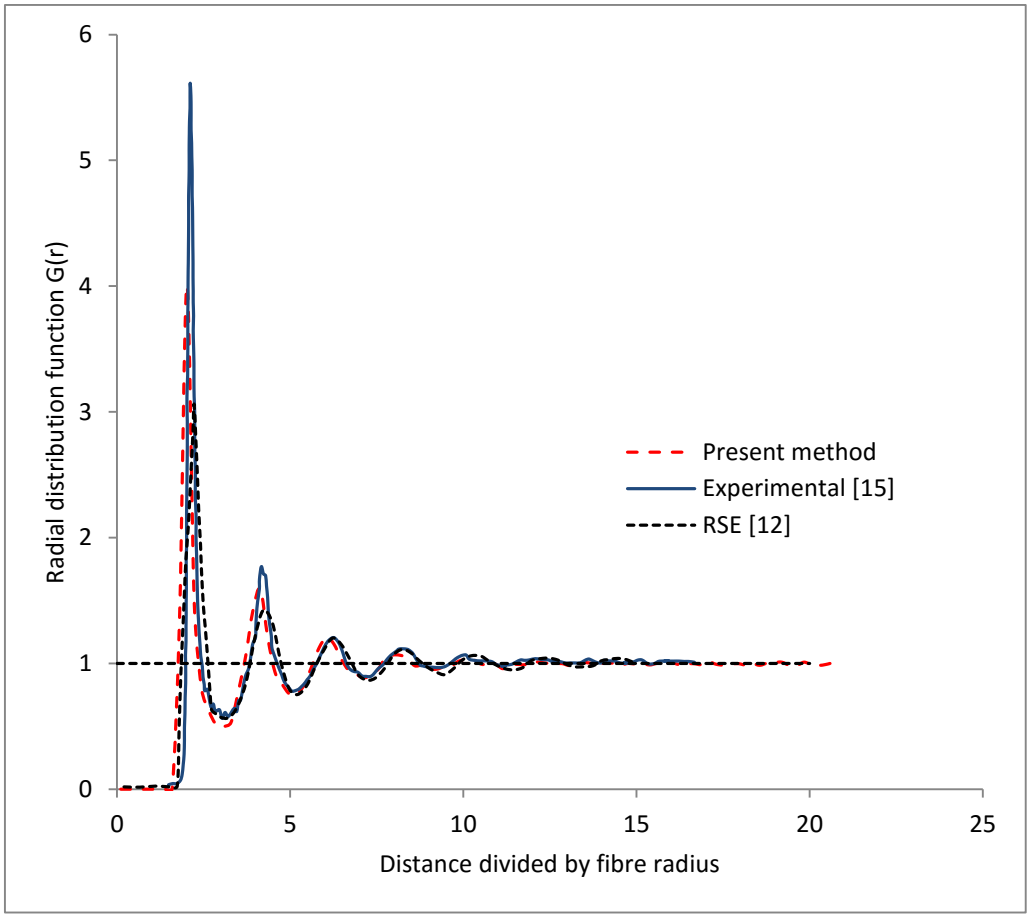

Fig.6. Radial distribution function for present method and compared with experimental RSE method.

4. Prediction of mechanical properties

As done for other algorithms [12, 15], the present algorithm is used to generate the RVEs of the transverse section of a composite laminae. The effective elasticity from the properties of their constituents is then evaluated by finite element models.

4.1 Finite element analysis

In this paper, the material that has been chosen to study is E-glass/MY750/HY917/DY063, consisting of E-glass fibres and epoxy resin as matrix. The properties have been reported in the World Wide Failure Exercise (WWFE) [22] and used by [12, 13]. Both the matrix and the fibre are treated as isotropic for the 2D model. The elastic properties of the fibre and the matrix are E_f=74 GPa, v_f=0.2 and E_m=3.35 GPa, v_m=0.35, respectively.

Finite element (FE) analysis was carried out using ABAQUS [23] under plane strain condition. In the ABAQUS model both the matrix and the fibres were meshed using free meshing technique with quad-dominated element shapes. The two-dimensional 4-node bilinear plane strain quadrilateral elements (CPE4) were chosen to mesh the fibre and the matrix. There were also a relatively small amount of 3-node linear plane strain triangle elements (CPE3) due to the free meshing technique used. Since each model has about 500 fibres, it is difficult and time consuming to generate each RVE manually. Therefore, python scripts have been written to generate and distribute fibres in the FE models of the RVEs in ABAQUS [23]. Twenty RVEs spatial distributions with V_f=60% were generated, each containing approximately 55,000 elements.

Periodic boundary conditions were applied on the RVEs to ensure the compatibility of strain and stress at macro level, similar to those used by [12, 24]. These consist of a series of constrains in which, the deformation of each pair of nodes on the opposing edge of the RVE were subject to the same amount of displacements, *i.e.*:

$$u_{23} - u_{v2} = u_{14} - u_{v1} \quad (7)$$

$$u_{43} - u_{v4} = u_{12} - u_{v1} \quad (8)$$

where u_{ij} is the *y* or *z* displacement of nodes on the edges and u_{vi} is the displacement of vertex node, *i*. Fig.7a and 7b show the periodic boundary conditions for tension and shear, respectively. Nodes in Eqs. (7) and (8) are connected by the "equation" constrains available in ABAQUS [23] and python scripts are used to implement these equations into the ABAQUS model. E_2 and v_{23} are determined by applying a horizontal displacement on node *2* while to determine E_3 and v_{32} a vertical displacement is applied on node *4*, as shown in Fig. 7a. G_{23} is determined by applying a horizontal displacement on node *4*, as shown in Fig. 7b.

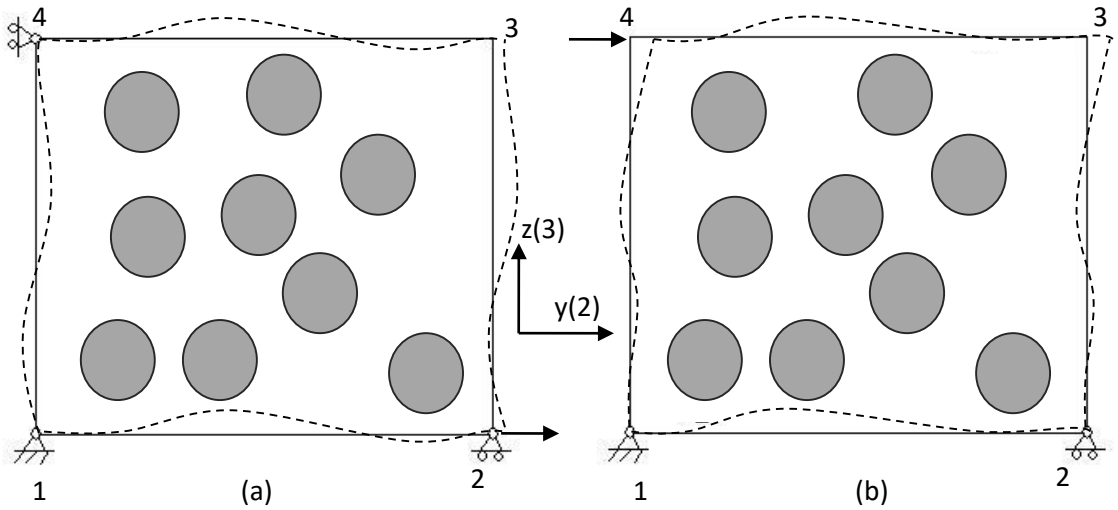

Fig.7. Periodic boundary constraints applied to the RVEs: (a) Tension, and (b) Shear.

The elastic properties were evaluated based on volumetric homogenisation procedure using the following equations [13]:

$$E_k = \frac{\sum_{i=1}^{N} \sigma_{kk}^i A^i}{\sum_{i=1}^{N} \varepsilon_{kk}^i A^i} \quad \varepsilon_{jk} = -\frac{\sum_{i=1}^{N} \varepsilon_{kk}^i A^i}{\sum_{i=1}^{N} \varepsilon_{jj}^i A^i} \quad G_{23} = -\frac{\sum_{i=1}^{N} \sigma_{23}^i A^i}{\sum_{i=1}^{N} \varepsilon_{23}^i A^i}, \tag{9}$$

where N is the total number of FE elements in the RVE, σ_{kk}^i and ε_{kk}^i are the average k-components of stress and strain of element i respectively, and A^i is the area of element i.

4.2 Analysis and results

The pattern of stress distribution in the RVEs is examined first. To this end, a displacement of 3 μm is applied on the RVEs for both tension and shear cases (see Fig.7). The von Mises stress contour plot for a RVE is shown in Fig.8. The von Mises stress varies from 19.8 MPa to 2213 MPa under transverse tension while the stress varies from 6.98 MPa to 977.7 MPa under transverse shear, as illustrated in Fig.8. In addition, it seems that the most of the high stresses area are located at interfaces especially where the distances between fibres are small. This is mainly due to the large differences of the mechanical properties between fibres and matrix.

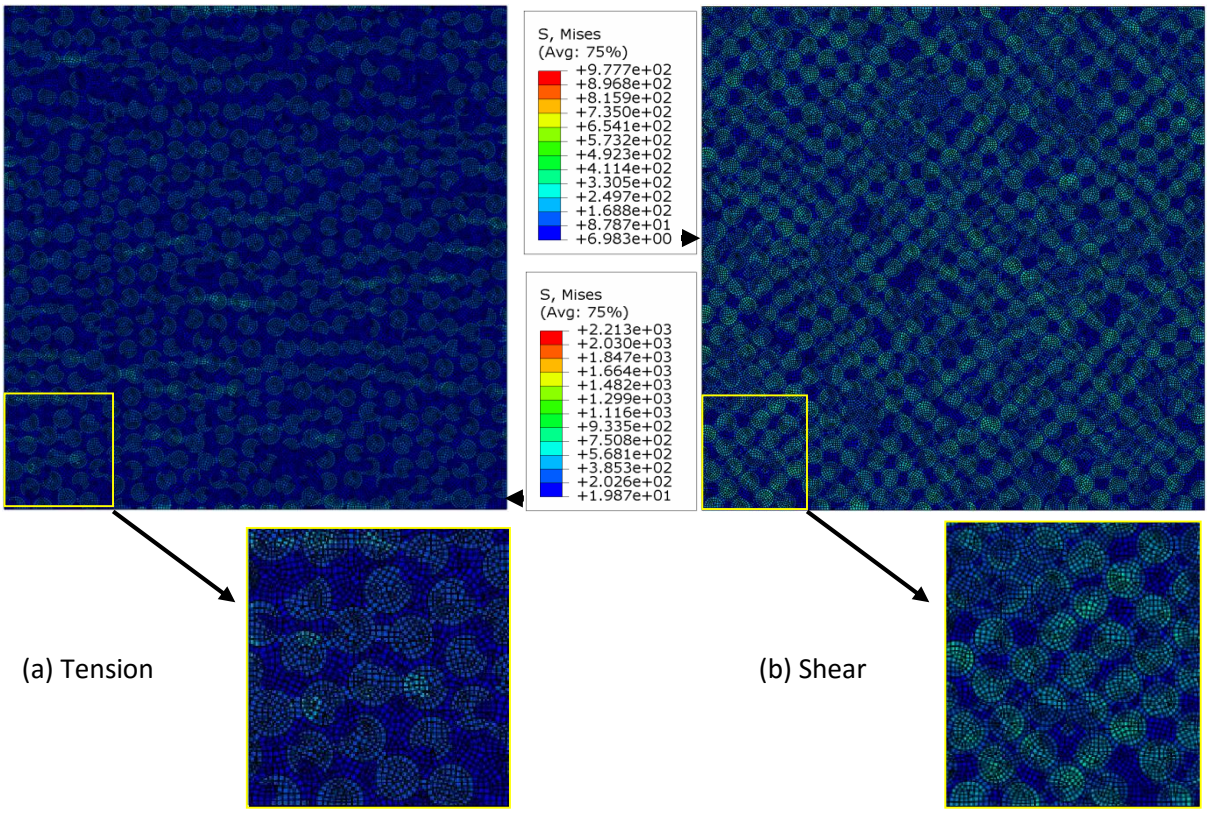

Fig.8. Von Mises stress distribution in a RVE under (a) tension and (b) shear

Effective properties are calculated numerically for the generated twenty microstructures using Eq. (9) and shown in Table 1, where their mean values and the standard deviations are also presented.

Table 1.Calculated effective properties

	E_2 (GPa)	E_3(GPa)	v_{23}	v_{32}	G_{23} (GPa)
Mean values	13.914	13.964	0.401	0.403	4.992
Standard deviations	0.661	0.794	0.031	0.022	0.251
Variation coefficient	0.048	0.057	0.077	0.056	0.050
Ref [13]	13.367	13.387	0.370	0.371	4.851
Ref [12]	13.047	13.068	0.405	0.405	4.673
Experimental [22]	16.2	16.2	0.4	0.4	5.786
Error (%, compared to experimental)	14.11	13.80	0.23	0.74	13.72

As seen from the table the average predicted Young's modulus and shear modulus of all RVEs are higher than those attained by [12, 13] and much closer to the experimental results, *i.e.*, the shear modulus shows 13.7% smaller than the experimental one in comparison with Yang's *et al.*, [12] prediction of 19% smaller.

As the material is assumed to be transverse isotropic in the x-z plane, the well-known consistent relationships which relate five independent elastic constants exist. The relationship between Young's modulus and Poisson's ratio is described as:

$$\frac{E_2}{\nu_{23}} = \frac{E_3}{\nu_{32}} \tag{10}$$

The transverse isotropy is determined by the following relationships:

$$E_2 = E_3,\ \nu_{23} = \nu_{32}, \bar{G}_{23} = \frac{E_2}{2(1+\nu_{23})}. \tag{11}$$

Table 2Proof of transverse isotropy

	$\frac{E_2\nu_{32}}{E_3\nu_{23}}$	$\frac{E_3}{E_2}$	$\frac{\nu_{23}}{\nu_{32}}$	$\frac{\bar{G}_{23}}{G_{23}}$
Mean values	1.002	0.996	1.005	0.995

Table 2 shows the transverse isotropy of Eqs. 10 and 11 are approximately satisfied using the predicted values in Table 1. It shows that all ratios are very close to 1 which concludes that the generated random fibre distributions have almost the same transverse isotropy as the real material.

5. Conclusions

A novel approach for generating random fibre distributions has been proposed and developed using the discrete element method (DEM). The approach is capable of generating random distributions of fibres with high volume fractions and any specified inter-fibre distances. Varied fibre diameters were assigned by extracting the experimentally measured diameter distribution. The reason for not using identical diameter is to avoid regular distribution of fibres and to ensure they are distributed randomly. The generated fibre distributions have been statistically analysed, and it was found that the approach was adequately capable of generating fibre distributions which was statistically equivalent to the real microstructure.

Finite element analysis was carried out to predict the effective elasticity of the generated microstructures, the results of which were compared with experimental and other methods. The predicted effective properties were found to be close to those measured from experiments and calculated using other algorithms. Especially, the predicted Poisson's ratios have shown excellent agreement with the experimental data. The developed algorithm will be particularly suitable for future DEM micromechanical modelling of the elasticity, strength as well as damage evolution of composite laminates. Also the method can be easily combined with conventional FEM micromechanical modelling of damage progression in composite materials.

References

1. González, C. and J. LLorca, *Multiscale modeling of fracture in fiber-reinforced composites.* Acta materialia, 2006. **54**(16): p. 4171-4181.
2. LLorca, J., C. González, J.M. Molina-Aldareguía, and C. Lópes, *Multiscale Modeling of Composites: Toward Virtual Testing… and Beyond.* JOM, 2013. **65**(2): p. 215-225.
3. Parıs, F., E. Correa, and J. Cañas, *Micromechanical view of failure of the matrix in fibrous composite materials.* Composites Science and Technology, 2003. **63**(7): p. 1041-1052.
4. Correa, E., V. Mantič, and F. París, *A micromechanical view of inter-fibre failure of composite materials under compression transverse to the fibres.* Composites Science and Technology, 2008. **68**(9): p. 2010-2021.
5. Swaminathan, S., S. Ghosh, and N. Pagano, *Statistically equivalent representative volume elements for unidirectional composite microstructures: Part I-Without damage.* Journal of Composite materials, 2006. **40**(7): p. 583-604.
6. Tsai, S.W. and E.M. Wu, *A general theory of strength for anisotropic materials.* Journal of Composite materials, 1971. **5**(1): p. 58-80.
7. Gusev, A.A., P.J. Hine, and I.M. Ward, *Fiber packing and elastic properties of a transversely random unidirectional glass/epoxy composite.* Composites Science and Technology, 2000. **60**(4): p. 535-541.
8. Trias, D., J. Costa, J. Mayugo, and J. Hurtado, *Random models versus periodic models for fibre reinforced composites.* Computational materials science, 2006. **38**(2): p. 316-324.
9. Hojo, M., M. Mizuno, T. Hobbiebrunken, T. Adachi, M. Tanaka, and S.K. Ha, *Effect of fiber array irregularities on microscopic interfacial normal stress states of transversely loaded UD-CFRP from viewpoint of failure initiation.* Composites Science and Technology, 2009. **69**(11): p. 1726-1734.
10. Buryachenko, V., N. Pagano, R. Kim, and J. Spowart, *Quantitative description and numerical simulation of random microstructures of composites and their effective elastic moduli.* International journal of solids and structures, 2003. **40**(1): p. 47-72.
11. Wongsto, A. and S. Li, *Micromechanical FE analysis of UD fibre-reinforced composites with fibres distributed at random over the transverse cross-section.* Composites Part A: Applied Science and Manufacturing, 2005. **36**(9): p. 1246-1266.
12. Yang, L., Y. Yan, Z. Ran, and Y. Liu, *A new method for generating random fibre distributions for fibre reinforced composites.* Composites Science and Technology, 2013. **76**: p. 14-20.
13. Melro, A., P. Camanho, and S. Pinho, *Generation of random distribution of fibres in long-fibre reinforced composites.* Composites Science and Technology, 2008. **68**(9): p. 2092-2102.
14. González, C. and J. LLorca, *Mechanical behavior of unidirectional fiber-reinforced polymers under transverse compression: microscopic mechanisms and modeling.* Composites Science and Technology, 2007. **67**(13): p. 2795-2806.
15. Vaughan, T. and C. McCarthy, *A combined experimental–numerical approach for generating statistically equivalent fibre distributions for high strength laminated composite materials.* Composites Science and Technology, 2010. **70**(2): p. 291-297.
16. Ismail, Y., Y. Sheng, D. Yang, and J. Ye, *Discrete element modelling of unidirectional fibre-reinforced polymers under transverse tension.* Composites Part B: Engineering, 2014. **73**: p. 118-125.
17. Itasca, *PFC2D-particle Flow Code (Itasca Consulting Group Inc., Minnesta).* 2003.
18. Illian, J., A. Penttinen, H. Stoyan, and D. Stoyan, *Statistical analysis and modelling of spatial point patterns*. Vol. 70. 2008: John Wiley & Sons.

19. Trias, D., J. Costa, A. Turon, and J. Hurtado, *Determination of the critical size of a statistical representative volume element (SRVE) for carbon reinforced polymers.* Acta materialia, 2006. **54**(13): p. 3471-3484.
20. MATLAB, *The MathWorks, Inc., 3 Apple Hill Dr., Natick, MA 01760.* 2012.
21. Pyrz, R., *Quantitative description of the microstructure of composites. Part I: Morphology of unidirectional composite systems.* Composites Science and Technology, 1994. **50**(2): p. 197-208.
22. Soden, P., M. Hinton, and A. Kaddour, *Lamina properties, lay-up configurations and loading conditions for a range of fibre-reinforced composite laminates.* Composites Science and Technology, 1998. **58**(7): p. 1011-1022.
23. ABAQUS, *Theory manual HKS Inc.* 2010.
24. Van der Sluis, O., P. Schreurs, W. Brekelmans, and H. Meijer, *Overall behaviour of heterogeneous elastoviscoplastic materials: effect of microstructural modelling.* Mechanics of Materials, 2000. **32**(8): p. 449-462.